Forestry An International Journal of Forest Research

Institute of Chartered Foresters

Forestry 2021; **94**, 127–140, doi:10.1093/forestry/cpaa018
Advance Access publication 3 June 2020

Models for predicting the within-tree and regional variation of tracheid length and width for plantation loblolly pine

Joseph Dahlen[1,*], Mohamad Nabavi[1], David Auty[2], Laurence Schimleck[3] and Thomas L. Eberhardt[4]

[1]*Warnell School of Forestry and Natural Resources, University of Georgia, 180 E Green St, Athens, Georgia, 30602, USA*
[2]*School of Forestry, Northern Arizona University, 200 East Pine Knoll Drive, Flagstaff, Arizona, 86011, USA*
[3]*Wood Science and Engineering, Oregon State University, 119 Richardson Hall, Corvallis, Oregon, 97331, USA*
[4]*Forest Products Laboratory, USDA Forest Service, One Gifford Pinchot Drive, Madison, WI, 53726, USA*

*Corresponding author: Email: jdahlen@uga.edu

Received 20 January 2020

Loblolly pine is a major fibre source for the pulp and paper industry. Here we developed the first nonlinear models to predict the within-tree and regional variation of tracheid length and width for planted loblolly pine. Data were obtained from macerated tracheids and near-infrared spectroscopy calibration models from trees sampled in 109 stands across the southeastern United States. The fixed effects for the final tracheid length model, which included cambial age, height of disk within tree, and physiographic region, explained 71 percent of the variation with root mean square error (RMSE) of 0.28 mm, while the fixed effects for the final tracheid width model explained 57 percent of the variation with RMSE of 1.4 μm. There was significant variation in tracheid properties across the growing regions. Tree maps showing within-tree variability in tracheid properties were produced. Five simulated scenarios were compared using the models developed, with mean tracheid dimensions calculated on a whole-tree basis at a first and second thinnings, and at final harvest. Also from the final harvest, the tops of trees, and outerwood chips produced during lumber manufacturing were also simulated. For the whole tree scenarios, both mean tracheid length and width increased with age, increasing from 2.24 mm and 40.5 μm (age 12), to 2.51 mm and 41.3 μm (age 18), and to 2.73 and 41.8 μm at age 25, respectively. The tops of the trees at age 25 had a mean tracheid length of 2.46 mm and a mean width of 41.0 μm, while the chips had a mean tracheid length of 3.13 mm and a mean width of 42.5 μm. Due to the models representing samples collected from across the southeastern United States, and their relatively high precision, they are suitable for incorporation into growth and yield systems allowing for prediction of tracheid properties.

Introduction

Loblolly pine (*Pinus taeda* L.) is the primary source of fibre for the pulp and paper industry in the southeastern United States. Roundwood accounts for approximately 80 percent of the softwood pulp produced in the region, with the remainder being chips from the outermost wood of logs removed during lumber manufacturing (Gray et al. 2018). Trees with diameter at breast height (d.b.h.) values ranging from 13 to 20 cm are pulpwood, while chip-n-saw and sawtimber trees, with a d.b.h. greater than 20 cm, are usually used for lumber. The tops of chip-n-saw and sawtimber trees are also used by the pulp and paper industry, as are trees of any size with visible defects that preclude their use in lumber, and these defects include sweep, crook, forks, and cankers from fusiform rust. The combined effects of improved genetic selection (McKeand et al. 2003) and enhanced silvicultural practices (Fox et al. 2007) have led to rapid growth, thereby allowing rotation ages to be decreased to 25 years or less, with site indices as high as 32 m (base-age 25) (Zhao et al. 2016). Accordingly, like other intensively managed conifer species, plantation-grown loblolly pine contains a large proportion of corewood (aka juvenile wood) (Burdon et al. 2004; White et al. 2009; Moore and Cown 2017).

Due to the radial and longitudinal variation in wood and fiber properties in a given loblolly pine tree stem, chips produced from the outermost wood of sawlogs will have different morphological fibre characteristics than pulpwood from thinning operations or tops of older sawtimber-sized trees. Both tracheid length and tracheid width increase radially (Lachenbruch et al. 2011, Hayatgheibi et al. 2019). Tracheid length varies by height within tree for a given cambial age, with the shortest tracheids at the base (Megraw 1985). For example, Megraw (1985) found that at stump height near the pith, tracheid length is approximately 1.5 mm, increasing to 2.25 mm higher in the stem. More recently, Schimleck et al. (2020) produced tree maps showing variation

in tracheid properties determined on solid samples using the SilviScan instrument (tracheid length not determined); for trees at age 22, tangential tracheid width increased from approximately 25 to 35 μm from pith to bark regardless of height. In loblolly pine and other "hard" pines (pine species that have high wood density: southern pine, radiata pine, red pine, lodgepole pine, etc.), the patterns of increasing tracheid length and tracheid width with height for a given cambial age (Megraw 1985; Schimleck et al. 2020) differ from specific gravity (SG), which is highest at the stump and decreases with height in the stem (Dahlen et al. 2018). Generally, most of the changes in wood properties with height in the tree occur within the first log at the base of the stem (stump to 5 m) (Burdon et al. 2004).

The changes that occur in tracheid dimensions due to the growth and maturation of trees results in tracheids with very different mechanical properties within the profile of the stem (Mott et al. 2002; Groom et al. 2002a, 2002b). Groom et al. (2002a) tested individual loblolly pine latewood tracheids in tension and found that at stump height, modulus of elasticity (MOE) of the tracheids increased from 6.6 to 24.6 GPa between cambial ages 5 and 48 (years). At the same height, and cambial age range, modulus of rupture (MOR) increased from approximately 400 to 1200 MPa. The within-tree variation in the mechanical properties of tracheids are a result of both the increase in the dimensions of the tracheids and a concomitant reduction in microfibril angle (MFA) (Brändström 2001).

Paper and paperboard properties (sheet density, tensile strength, tear strength, burst strength) are strongly influenced by tracheid length and tracheid width (Kibblewhite 1980; McKenzie 1994; Evans et al. 1997; Kibblewhite et al. 1997; Evans et al. 1999; Kibblewhite et al. 2003; Via et al. 2004; Pulkkinen et al. 2006). Collapsibility is a function of the ratio of tracheid width to the cell wall thickness, and since tracheids with thick walls tend to resist collapse, sheets with low density are formed (Kibblewhite et al. 1997; Kibblewhite et al. 2003). Although the shorter lengths and thinner walls of juvenile wood fibres may result in lower tear strength, burst strength is higher (Zobel and Sprague 1998); thus, while properties of paper produced from mature wood and juvenile wood can be quite different, paper produced from the latter is not necessarily inferior for specific product types.

Given within-tree changes in tracheid dimensions with cambial age and height, the development of predictive models for tracheid width and length would be of particular use to the pulp and paper manufacturing sector for informing procurement strategies. Combining models that predict tracheid dimensions, with knowledge of pits within the tracheids, would enable better links to tree physiology (Domec and Gartner 2002). However, developing robust models requires data from a large number of samples, and the measurement of tracheid dimensions is both time-consuming and expensive. Individual tracheids must first be separated through a slow and harsh chemical treatment (maceration), and then the length and width measured for each tracheid using an optical image analyser (Hirn and Bauer 2006). An alternative method for measuring tracheid width on solid samples relies on the SilviScan system, which measures the radial and tangential diameters of tracheids, with wall thickness and coarseness (being the weight per unit length) calculated from the tracheid diameters and density measurements collected using an X-ray densitometer (Evans 1994). Tracheid width and cell wall thickness are not directly comparable between solid samples and macerated samples because during chemical pulping tracheid width and cell wall thickness decrease due to associated losses of hemicelluloses and lignin (Scallan and Green 1975; Kibblewhite and Evans 2001; Çöpür et al. 2005). In contrast, tracheid length remains largely unaffected by chemical pulping (Paavilainen 1993). One solution for increasing the sample throughput of measuring tracheid length, which cannot be measured rapidly on intact radial samples, is to combine near-infrared (NIR) spectroscopy or hyperspectral imaging predictions with macerations, to provide rapid estimations of tracheid properties (Schimleck et al. 2004; Via et al. 2005). Nabavi et al. (2018) developed NIR calibrations for tracheid width and length collected from loblolly pine samples from across the southeastern United States and reported strong prediction statistics for tracheid dimensions.

In the current study, our primary goals were to: 1) develop predictive models of tracheid dimensions (i.e. length and width) as functions of cambial age, height along the stem, and physiographic region for loblolly pine harvested from plantations from across the southeastern United States; 2) build tree "maps" showing the within-tree variation in these properties; 3) calculate mean tracheid properties for different roundwood procurement scenarios across a rotation. Predictive models of tracheid dimensions are herein provided in a format that will allow their incorporation into growth and yield systems, facilitating more informed decision-making that can account for the variation in wood properties (Lindström 2002; Briggs 2010; Burkhart and Tomé 2012).

Methods

Sample locations and sample preparation

The loblolly pine samples analysed in this study were from the Wood Quality Consortium baseline study (Jordan et al. 2008; Antony et al. 2010; Nabavi et al. 2018); 109 stands were sampled from six physiographic regions of the southeastern United States: 1) Lower Coastal Plain (N = 32), 2) North Atlantic (N = 7), 3) Upper Coastal Plain (N = 12), 4) Piedmont (N = 16), 5) Gulf Coastal Plain (N = 16) and 6) Hilly Coastal region (N = 26) (Figure 1). Phosphorus fertilizer was applied on deficient sites at stand establishment, but otherwise there was no fertilization or competition control. From each stand, three trees were felled, one tree from the mean diameter class, and one tree from each of the classes 50 mm above and below the mean diameter class. In total, 268 trees produced samples that were suitable for this study. Wood disks, 25 mm thick, were cut at approximately 1.5 m intervals starting from the stump up to a top diameter of 25 mm, with the second disk being collected at breast height (1.37 m above ground-level). Each disk typically yielded two pith-to-bark radial strips cut to 12 mm high by 12 mm wide which were then dried to approximately 12 percent moisture content. The radial strips obtained from the disks that were not blue-stained (N = 1842) were scanned on a FOSS NIRSystems Model 5000 scanning spectrophotometer (FOSS NIRSystems, Inc., Laurel, MD) with a static diffuse-reflectance module. Spectra were obtained from the radial-longitudinal face every 10 mm. The annual rings were counted for each 10-mm interval to determine the mean cambial age for each 10-mm section that would later be cut from

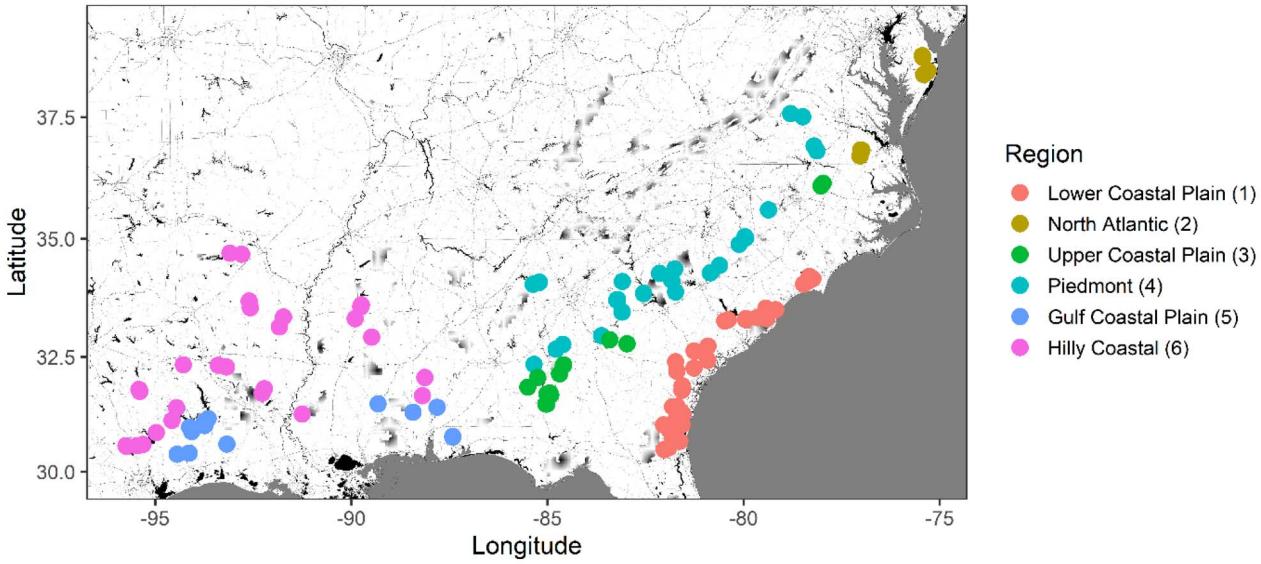

Figure 1 Map of the stands sampled from across the southeastern United States.

the radial strip. A total of 11 428 10-mm intervals (sections) were scanned on the NIR spectrometer (Nabavi et al. 2018).

A total of 2018 wood sections were macerated after being selected using the Duplex (Snee 1977) sample selection algorithm (Nabavi et al. 2018). The wood sections selected for maceration were cut using a razor blade into smaller (ca. 2 mm) pieces and then macerated with 20 mL of 50 percent hydrogen peroxide, 30 mL of water, and 50 mL glacial acetic acid at 60°C for 48 hours (Franklin 1945). The tracheids were separated from the pulping chemicals using a Buchner funnel and filter paper, rinsed with approximately 1.9 L of water, and then the rinsed tracheids were washed into a beaker, separated by gently shaking, and diluted with water to a total approximate volume of 1 L. The resultant fiber suspensions were then analysed using a TechPap MorFi Compact Fiber & Shive Analyzer with a 4-µm resolution camera (Techpap SAS, France) where for each sample approximately 2500 tracheids were measured. The length-weighted tracheid length and the width-weighted tracheid width were calculated based on the distribution of tracheids measured which minimizes the effect of cut tracheids (Carvalho et al. 1997). Length-weighted tracheid length is calculated by:

$$L_l = \frac{\Sigma_{n_i l_i^2}}{\Sigma_{n_i l_i}} \# \quad (1)$$

where L_l is length-weighted tracheid length, n_i is number of tracheids in the ith class, and l_i is the mean length of the ith class (Carvalho et al. 1997), width-weighted tracheid width was calculated using the same equation but substituting width for length.

Partial least squares (PLS) regression models were constructed on the calibration dataset (N = 1020) and their performance checked against the validation set (N = 998). The calibration model for tracheid length applied to the validation set had R^2 = 0.87 and standard error of prediction = 0.23 mm. The calibration model for tracheid width applied to the validation set had R^2 = 0.61 and standard error of prediction = 1.6 µm, which was within the measurement error of an individual tracheid for the system (± 2 µm). The values for tracheid length and tracheid width of the remaining 9410 samples were predicted from these models (Nabavi et al. 2018).

Model development and statistical analysis

Models, statistical analyses and associated graphics were done in the R statistical programming environment (R Core Team 2019) using the RStudio interface (RStudio 2019). Data wrangling was done using the tidyverse series of packages (Wickham 2017), and data visualizations were produced using ggplot2 (Wickham 2009). Nonlinear mixed-effects models were developed using the nlme library (Pinheiro et al. 2016); those were compared using AIC values, likelihood-ratio tests, fit indices (R^2) of the fixed, and fixed plus random (stand, tree) components of the models, and root mean square error (RMSE) values. All models were developed iteratively, keeping only those parameters with p-values less than or equal to 0.05 in the models. Serial correlation (autocorrelation) due to the repeated measurements (multiple measurements per disk) was addressed by adding a first order continuous autoregressive AR(1) autocorrelation structure (Pinherio and Bates 2000). Tree maps were produced using the gstat (Pebesma 2004; Gräler et al. 2016), raster (Hijmans 2016), and spatstat (Baddeley et al. 2015) packages.

Tracheid length model development

An important part of the modeling exercise was to identify a suitable model form that adequately represented the available data, but could also be applied outside the data range. For loblolly pine, the four-parameter logistic function has previously been used for

modeling the variation of SG with cambial age (Mora et al. 2007; Antony et al. 2011; Dahlen et al. 2018). This model form was considered here, but the model tends to reach an asymptote at relatively young cambial ages. While a different species, Mäkinen et al. (2007) found that tracheid length for Norway spruce (*Picea abies* (L.) Karst.) continues to increase for 60 years. Since the material in this study originated from short-rotation plantations less than 30 years old, we looked for a model form where the response gradually increased over time to account for increases in tracheid length at cambial ages beyond the range of the data. Such a model form reflects a balance between the available data and the available literature on tracheid length. As such, we used a 3-parameter curve with an inflection point:

$$length = \beta_0 \left(1 - e^{-\beta_1 CA^{\beta_2}}\right) \tag{2}$$

where length is the tracheid length for an annual growth ring at a particular cambial age, CA is the cambial age (ring number from the pith), β_0 is the model asymptote, and the β_1 and β_2 parameters determine how fast the model reaches the asymptote (Ratkowsky 1990). Although this model form reaches an asymptote, the length of time it takes to do so exceeds the cambial age range in our data and thus was considered a suitable model form for tracheid length in this study.

Considering both fixed and random effects, the base model was:

$$length_{ijkl} = (\beta_0 + b_{0i} + b_{0ij}) \left(1 - e^{-\beta_1 CA_{ijkl}^{\beta_2}}\right) \tag{3}$$

where length and cambial age represent the *l*th annual ring of the *k*th disk from the *j*th tree at the *i*th site. The fixed effects parameters are β_0, β_1, and β_2, and the random effects for the model, b_{0i} and b_{0ij}, represent the nested random effects of the asymptote parameter (β_0) at the site and tree levels, respectively. Because tracheid length varies with height within a tree, i.e. increasing at the pith with increasing height (Megraw 1985), the effect of disk height (DH) was incorporated into equation 4 as follows:

$$length_{ijkl} = \left(\beta_0 + b_{0i} + b_{0ij}\right)\left(1 - e^{-(\beta_1 + \alpha_1 \log(1+DH)) CA_{ijkl}^{\beta_2 + \alpha_2 \log(1+DH)}}\right) \tag{4}$$

where α_1 is the fixed effect that varies β_1 and α_2 is the fixed effect that varies β_2 by disk height. The nonlinear effect of disk height was incorporated into the model by taking the natural logarithm of disk height (in meters). For each disk height, 1 m was added to each value to prevent negative infinity values and to reduce the slope of the natural log effect that occurs with values below 1. Moore et al. (2014) employed a similar procedure when modelling MFA for radiata pine (*Pinus radiata* D. Don). The effect of region was incorporated into the disk height model (equation 4) by allowing the β_0 term to vary by region (equation not shown).

Tracheid width model development

For tracheid width, the three-parameter logistic function (Ratkowsky 1990) was selected:

$$width = \frac{\beta_0}{1 + e^{\left(\frac{\beta_1 - CA}{\beta_2}\right)}} \tag{5}$$

where width is the mean ring tracheid width for a particular growth ring, β_0 is the asymptote as cambial age approaches infinity, β_1 the inflection point, and β_2 a scale parameter. Considering both fixed and random effects, the base model form was:

$$width_{ijkl} = \frac{\beta_0 + b_{0i} + b_{0ij}}{1 + e^{\left(\frac{\beta_1 - CA_{ijkl}}{\beta_2}\right)}} \tag{6}$$

where $width_{ijkl}$ is the mean tracheid width in each annual growth ring, CA_{ijkl} is the cambial age of the lth annual ring of the kth disk from the jth tree at the ith site. The random effects for the model are b_{0i} and b_{0ij}, and represent the nested random effects of the asymptote parameter (β_0) at the site and tree levels, respectively. Because loblolly pine tracheid width varies by height within a tree, the effect of disk height was incorporated into the model as follows:

$$width_{ijkl} = \frac{\beta_0 + b_{0i} + b_{0ij} + \alpha_0 \log(1 + DH)}{1 + e^{\left(\frac{\beta_1 - CA_{ijkl}}{\beta_2}\right)}} \tag{7}$$

where α_0 is the fixed effect that varies the β_0 parameter with the log of disk height plus 1 m added as was done for the tracheid length models. The effect of region was incorporated into the disk height model (equation 7) by allowing the β_0 term to vary by region.

Tree property map development

Within-tree wood property maps were produced following the procedures described by Auty et al. (2014) and Dahlen et al. (2018). For intra-tree tracheid property variation, we predicted the height of the tree from age 1 to 30 years using the dynamic model developed by Diéguez-Aranda et al. (2006) for loblolly pine:

$$Y = \frac{26.14 + X_0}{1 + \frac{1455}{X_0} * t^{-1.107}} \tag{8}$$

where Y is the predicted height at age t, and X_0 is:

$$X_0 = 0.5 * \left(Y_0 - 26.14 + \sqrt{(Y_0 - 26.14)^2 + 4 * (1455 * Y_0 * t_0^{-1.107})}\right) \tag{9}$$

where Y_0 is the site index (m) and t_0 is the base age (25 years). The site index we used to build the model was 23.7 m, which is the average site index of the stands in the current study. The diameter inside bark at breast height was predicted using the ring width model developed by Dahlen et al. (2018):

$$RW = \frac{108.64 - 1.108DH}{8.66 + CA} \quad (10)$$

where RW is ring width in mm. To utilize taper models to predict the diameter at different height levels, the diameter inside bark at breast height was converted to diameter outside bark using the relationship developed by Dahlen et al. (2018):

$$DOB = 1.073 * DIB \quad (11)$$

where DOB is diameter outside bark (cm), and DIB is the diameter inside bark (cm) ($R^2 = 0.99$, RMSE = 0.62 cm). The diameter of the tree was predicted for each sequenced height level using the model generated by Bullock and Burkhart (2003) for loblolly pine with its original English units (inches, feet):

$$DOB = abs\left(\frac{d.b.h^{4.1697}}{-0.9468}\right)^{\frac{1}{4.3397}} * abs\left(Log\left(1 - 0.8819 * \left(\frac{(H-h)^{2.883}}{H^{2.4610}}\right)\right)\right)^{\frac{1}{4.3397}} \quad (12)$$

where abs is the absolute value, d.b.h. is the diameter at breast height in inches, H is total height in feet, and h is each successive height level in feet. The site index tree height, DIB to DOB, and taper models provided annual height and taper information for ages 1 to 30 throughout the entire stem. The tracheid dimensions tree map thus generated shows the yearly values of tracheid length and width at each specific combination of cambial age and height. To produce a smoothed map showing the within-tree variation in tracheid dimensions, the data were interpolated using an inverse-distance weighted interpolation algorithm with a 25 by 25 kernel (Baddeley et al. 2015).

Mean tracheid properties during a rotation

The modelled annual within-tree tracheid length and tracheid width dataset was used to calculate the mean tracheid dimensions for five simulated roundwood procurement scenarios that follow where pulp mills obtain raw materials in the southeastern United States. First thinning typically occurs at age 12 when trees have reached pulpwood size (≥15 cm d.b.h.), with the whole tree up to a 5-cm top being sent to the pulp mill (scenario #1). Second thinning use the same diameter criteria as first thinnings and typically occur at age 18; most material is sold as pulpwood, but some material is large enough as chip-N-saw logs for lumber production, and is excluded (scenario #2). At the final harvest age (i.e. rotation age) considered here, 25 years, material can be sold to a pulp mill in three different ways: whole trees that contain defects are sold as pulpwood (scenario #3), similar to the first two scenarios; tops of trees obtained from a clearcut, with wood up to a 13 cm diameter being sent to lumber facilities, and the remaining wood to a 5 cm diameter sold as pulpwood (scenario #4); and finally, taking into consideration the fibre properties from the outerwood of sawlogs, the outermost wood of sawlogs is removed via a chipper-canter headrig and the resultant chips are sold to a pulp mill (scenario #5). Because they are exclusively outerwood, these chips have different fibre properties than their whole-tree or tops counterparts.

To calculate the mean tracheid length and width values for the first three scenarios, the total volume of the tree from the stump (0.15 m) to a 5 cm diameter top (2.5 cm radius, see Figure 2) was calculated. The tracheid property values at each height and cambial age combination were weighted by the volume of the annual ring compared to the overall volume. The weighted tracheid length and width values were then summed for each respective height and cambial age combination, giving the mean tracheid length and width values for the tree. For the 4th scenario, the minimum small end diameter for sawtimber was 13 cm (6.5 cm radius), thus, the tops were from the height at which this occurred to a 5 cm top. For the 5th scenario, the sawlog was assumed to be from the stump height (0.15 m) to the merchantable height (>13 cm). The sawlog was split into 5.2-m logs, or in the case of the third log, the remaining length from the top of the second log to the 13 cm diameter merchantable height. The small end diameter for each log was assumed to be processed into lumber, and any material above the small end diameter was assumed to be chipped. The volume of the chips and the weighted length and width of the chipped materials were calculated as described above.

Results

When averaged across all rings, mean tracheid length was 2.4 mm, with a standard deviation (SD) of 0.52 mm (Table 1). For tracheid width, the mean was 41.0 μm (SD = 2.08 μm). Generally, the regions closer to the southern coast, specifically the Lower Coastal, Upper Coastal, and Gulf Coastal Plains, had greater mean tracheid lengths and tracheid widths. Due to the greater ranges in the data for these regions, the standard deviations were higher than those for the other regions; the lowest variations in the data were in the North Atlantic and Piedmont regions. Tracheid length ranged from a minimum of 0.8 mm to a maximum of 4.0 mm. Note that values outside this range were measured on individual tracheids. The measurements provided here are the weighted lengths (and widths) determined from the frequency distribution of individual tracheid length (and width) values measured using the fibre analyser to minimize the effects of fines and cut tracheids on the data.

The summary tables for the model parameters are shown in Table 2. Summaries of the fit indices and error statics for these models are shown in Table 3. At the same cambial age, tracheid length and width both increased with disk height. Accordingly, the fit indices were higher for the hierarchical effects (fixed, stand, tree) when disk height was included in the model. Tracheid length and width varied by region, and thus the fit indices further improved when including region in the model.

Tracheid length increased rapidly for the first 8 growth rings then continued to gradually increase over time. The base tracheid length model (equation 3) did not include disk height (or region) and explained 55 percent of the variation in tracheid length (fixed effects only), and the RMSE was 0.35 mm. Allowing

Table 1 Summary of tracheid property values overall and by region (see Figure 1 for stand locations in each region).

Region[1]	# Stands	Tracheid Length (mm)				Tracheid Width (μm)			
		Mean	Min	Max	SD	Mean	Min	Max	SD
1	32	2.5	0.8	4.0	0.55	41.5	33.2	48.9	2.09
2	7	2.2	0.9	3.2	0.45	39.9	31.9	46.2	1.99
3	12	2.4	1.0	3.7	0.50	41.1	32.8	48.6	2.08
4	16	2.2	1.1	3.7	0.48	40.4	32.6	46.2	1.95
5	16	2.5	0.9	3.9	0.55	41.3	33.2	47.6	2.13
6	26	2.4	1.1	3.6	0.49	40.7	32.6	47.2	1.95
Overall	109	2.4	0.8	4.0	0.52	41.0	31.9	48.9	2.08

[1]Region 1 = Lower Coastal Plain; Region 2 = North Atlantic; Region 3 = Upper Coastal Plain; Region 4 = Piedmont; Region 5 = Gulf Coastal Plain; Region 6 = Hilly Coastal

Table 2 Parameter estimates for the tracheid length and tracheid width models.

Property	Parameter	Model[1]	
		Base (eq. 3)	Disk Height (eq. 4)
Tracheid length	β_0	4.050 (0.085)	3.828 (0.061)
	β_1	0.355 (0.006)	0.193 (0.003)
	β_2	0.491 (0.009)	0.656 (0.010)
	α_1	-	0.100 (0.003)
	α_2	-	−0.070 (0.003)
		Base (eq. 6)	Disk Height (eq. 7)
Tracheid width	β_0	42.777 (0.074)	41.729 (0.083)
	β_1	−4.525 (0.107)	−4.740 (0.116)
	β_2	3.270 (0.052)	3.448 (0.058)
	α_0	-	0.602 (0.019)

[1]Standard errors for parameters in parentheses

Table 3 Fit indices and model errors for the tracheid length and tracheid width models.

Property	Model[1]	AIC	Fit indices (R^2)			Model errors[2]		
			Fixed	Stand	Tree	E	RMSE	|E|%
Tracheid	Base	838	0.55	0.65	0.68	-0.004	0.347	11.55
Length	DH	-2448	0.68	0.77	0.80	-0.001	0.294	10.03
	Region	-2485	0.71	0.76	0.80	-0.006	0.279	9.52
Tracheid	Base	36 667	0.46	0.57	0.61	0.028	1.517	2.89
Width	DH	35 735	0.52	0.62	0.66	0.028	1.438	2.76
	Region	35 666	0.57	0.63	0.68	0.014	1.356	2.69

[1]Base model does not include disk height or region, DH = disk height model. [2]Mean error (E), root mean square error (RMSE), and mean percentage error (|E%|) are calculated from the fixed part of each model.

tracheid length to vary by height (disk height model, equation 4) improved the percent of the variation explained to 68 percent (fixed effects only) and reduced the RMSE to 0.29 mm. This model also had a lower AIC and higher log-likelihood than the base model ($p < 0.0001$). The asymptote (β_0) was 3.82 mm which is reasonable given the data (Table 2) and previous work in loblolly pine (Megraw 1985). The stand-level random effects explained an additional 9 percent of the variability in the data, and tree-within-stand explained a further 3 percent of the variation. A scatterplot showing the variation of tracheid length with cambial age and disk height in the stem is shown in Figure 3. Allowing the asymptote term (β_0) to vary by region yielded a significantly

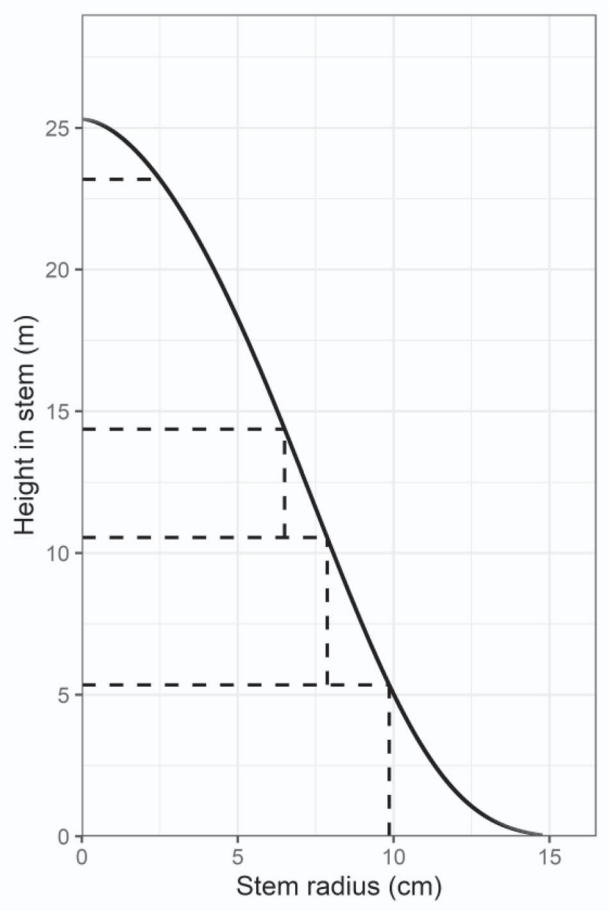

Figure 2 Diagram for scenarios #3, #4 and #5 at age 25. Scenario #3 considered the whole-tree to a 2.5 cm radius top. Scenario #4 represented the tracheid properties from the tops of the trees from 6.5 cm to 2.5 cm radius. Scenario #5 represented the tracheid properties of the chips produced during lumber manufacturing from the outermost wood of the logs at age 25. The solid line indicates the taper of the tree and the dotted lines represent the distinction between the various scenarios.

improved model versus the disk height model ($p < 0.0001$). The Gulf Coastal Plain (region 5) had the highest tracheid length asymptote (4.07 mm) versus the Lower Coastal Plain (region 1) and Upper Coastal Plain (region 3) (3.85 mm). The Hilly Coastal region (6) had a higher asymptote (3.72 mm) versus the North Atlantic (region 2) and the Piedmont (region 4) (3.53 mm). The incorporation of region improved the percent variation explained to 71 percent (fixed effects) and reduced the RMSE to 0.28 mm.

Tracheid width also increased rapidly for approximately 8 years, then gradually increased to an asymptote at approximately 15 years. The base tracheid width model (equation 6), that did not include a term for disk height, explained 46 percent of the variation (fixed effects only), with an RMSE of 1.5 µm. Allowing tracheid width to vary by height (disk height model, equation 7) improved the variation explained to 52 percent (fixed effects only) and reduced the RMSE to 1.4 µm, a significant improvement over model 1 according to AIC and a likelihood-ratio test ($p < 0.0001$). The asymptote (β_0) was 41.7 µm (Table 2) which is reasonable based on reported tracheid widths in loblolly pine (Schimleck et al. 2020). The stand-level random effects accounted for an additional 10 percent of the variability in tracheid width, and tree-within-stand explained a further 4 percent of the variation. A scatterplot showing the variation of tracheid width with cambial age and height in the stem is shown in Figure 4. Allowing the asymptote term (β_0) to vary by region yielded a significantly improved model versus the disk height model ($p < 0.0001$). The Lower Coastal Plain (region 1), Upper Coastal Plain (region 3), and Gulf Coastal Plain (region 5) had the highest tracheid width (42.5 µm) versus the other regions (41.8 µm). The incorporation of region improved the percent variation explained to 57 percent (fixed effects), however the RMSE was not affected (1.4 µm).

The modelled tree maps for both tracheid length and width for a mean tree across all regions from this study are shown in Figure 5. The maps illustrate that for tracheid length, the variability in height is largely restricted to the first 5-m log and then only gradual changes occur due to height. Radial variability, due to cambial age, is large for tracheid length throughout the data range. in contrast, for tracheid width, the variability with height is minimal and most of the variability is due to cambial age. Both maps show that tracheid properties generally increase with height and that length increases relatively more than width.

For the five simulated scenarios (Table 4), both mean tracheid length and width increase with age as follows: 2.24 mm and 40.5 µm (age 12, scenario #1), 2.51 mm and 41.3 µm (age 18, scenario #2), and 2.73 mm and 41.8 µm (age 25, scenario #3). The tops of the trees at age 25 (scenario #4) had a mean tracheid length and width of 2.46 mm and 41.0 µm, respectively, while chips obtained from the outerwood of sawlogs had a mean tracheid length of 3.13 mm and a mean tracheid width of 42.5 µm. At age 25, the longest tracheids (weighted) are found at 4.0 m in height (3.28 mm), while the widest tracheid (weighted) are found at 13.8 m in height (43.2 µm).

Discussion

The models presented are the first nonlinear models developed for tracheid length and width of loblolly pine to be reported in the literature. The radial and longitudinal variation in tracheid dimensions in this study are consistent with previous work on plantation-grown loblolly pine (Megraw 1985) and with general trends reported for softwoods (Cown and Kibblewhite 1980; Lindström 1997). Variation in tracheid length was captured in a model that predicted tracheid length as a function of cambial age; the fit for the model was improved by including the random effects of both stand and tree. Incorporating disk height gave a better fit over the base model (Figure 3), which was also improved by including the random effects. The increase in predicted values with height in the tree are shown in Figures 3-5. The model for tracheid length had better prediction accuracy ($R^2 = 0.55$) than the corresponding tracheid width model ($R^2 = 0.46$); this carried over to all permutations with the inclusion of disk height and physiographic region in the model, and the random effects of stand and tree. The poorer performance for the tracheid width model can be attributed to various factors, including the narrower range of values for tracheid width, and limits to the optical resolution of

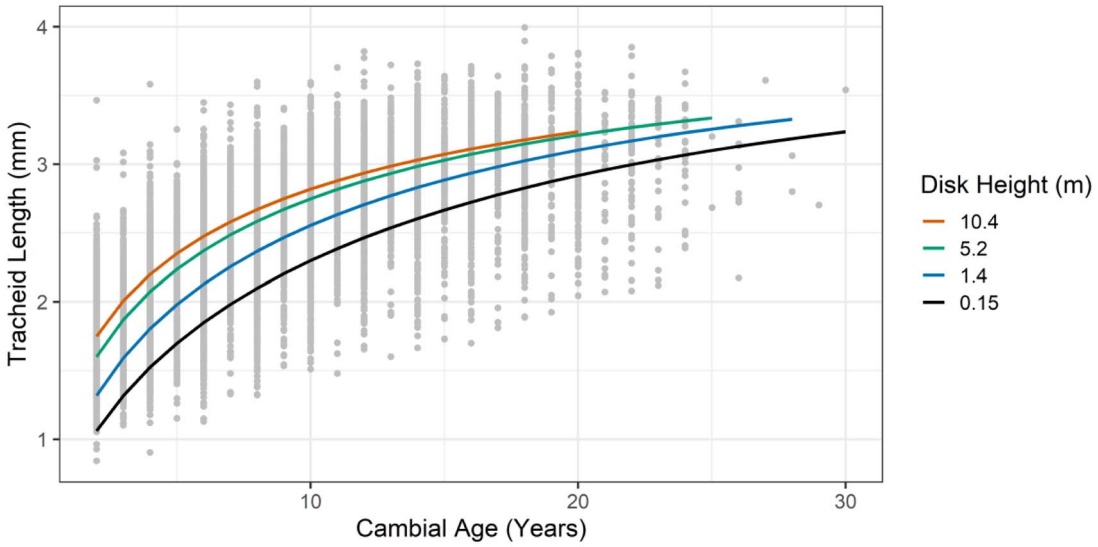

Figure 3 Variation in loblolly pine tracheid length by cambial age and disk height within tree. Lines represent predictions from equation 4 at the following disk heights: 0.15 m, 1.4 m, 5.2 m, and 10.4 m.

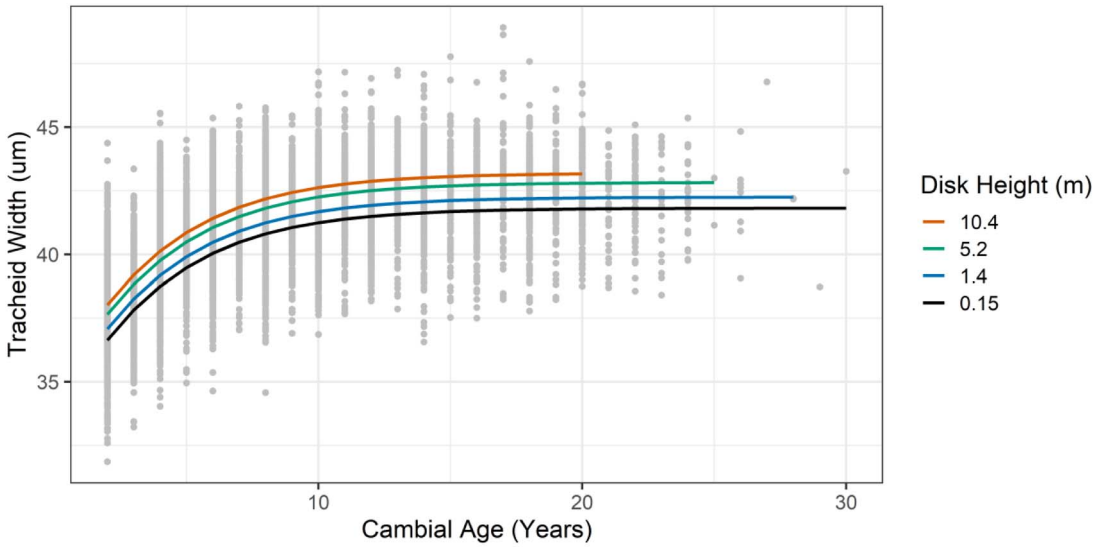

Figure 4 Variation in loblolly pine tracheid width by cambial age and height within tree. Lines represent the predictions from equation 7 at the following disk heights: 0.15 m, 1.4 m, 5.2 m, and 10.4 m.

the fiber analyzer, as well as uncontrollable variability in taking measurements on macerated tracheids. In regard to the last factor, the tracheid width measurement represents both tangential and radial width of the tracheids. Tangential tracheid diameter is relatively constant within an annual ring whereas radial diameter varies between the earlywood and latewood (Evans 1994). The orientation of the fibers in the optical path during the measurement could impact the width value depending upon whether the tangential view, radial view, or an intermediate view is measured. The ability to differentiate between radial diameter and tangential diameter may improve future modeling efforts, but doing so would present some technical obstacles and exorbitantly increase sample measurement time. Also, as mentioned earlier, the pulping of fibers impacts the measurement of width but not length (Paavilainen 1993).

Megraw (1985) presented results based on the variation of measured tracheid dimensions with cambial age and disk height, but no models were reported. Our models allow for their inclusion in growth and yield prediction systems, as well as procurement model systems that predict within-tree wood properties based on age and tree size. The models developed represent the variation in the available data while accounting for the limitations in the

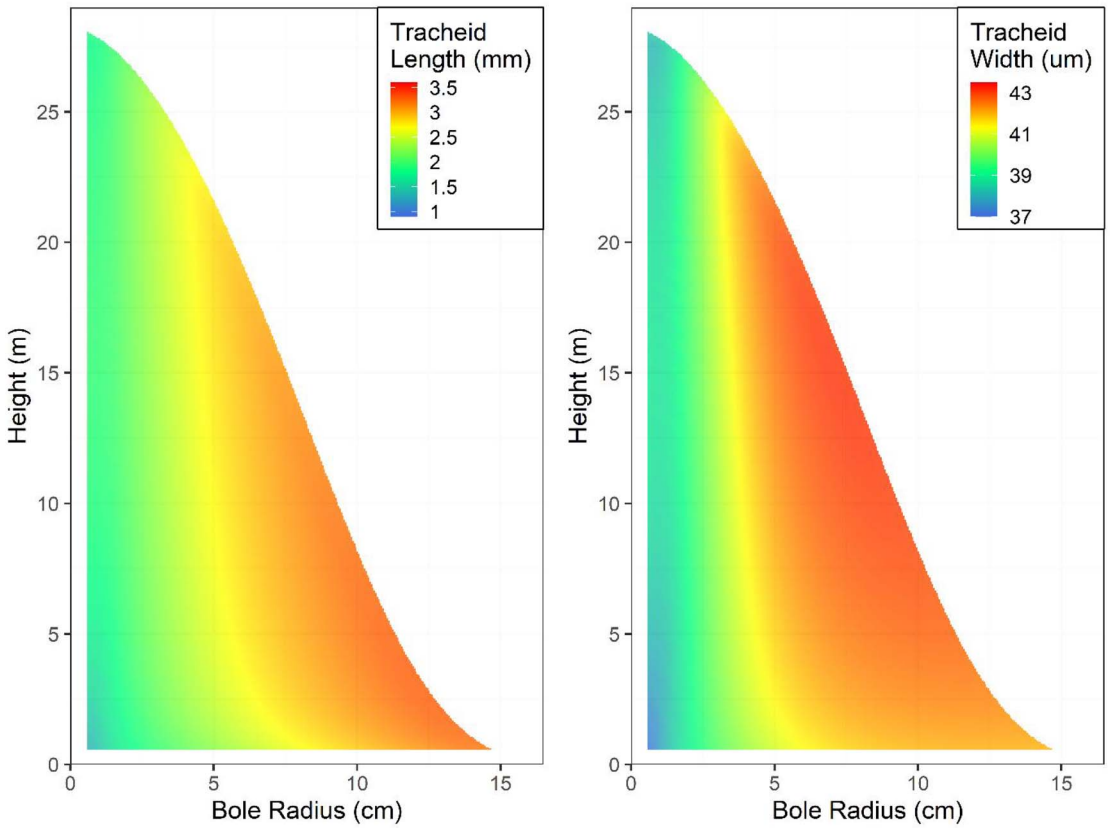

Figure 5 Modelled within-tree wood properties maps for tracheid length (left) and tracheid width (right).

Table 4 Tracheid length and width values during a rotation for five timber product scenarios across a 25-year rotation.

Scenario	Age	Pulpwood resource	Volume (m^3)	Tracheid Length (mm)	Tracheid Width (μm)
#1 First Thinning	12	Whole-tree	0.102	2.24	40.5
#2 Second Thinning	18	Whole-tree	0.25	2.51	41.3
#3 Final Harvest	25	Whole-tree	0.468	2.73	41.8
#4 Final Harvest	25	Tops only	0.065	2.46	41.0
#5 Final Harvest	25	Outerwoodchips	0.105	3.13	42.5

data. Here, tracheid length reached an asymptote at 3.83 mm before including height effects. Other work suggests that tracheid length will not reach an asymptote or will do so much later than we have shown, and thus the question arises of how accurate the models are when extrapolated beyond the range of the data (Gogoi et al. 2018). For example, in Norway spruce, Buksnowitz et al. (2010) found that tracheid length reaches asymptotic values after 100 years, with rapid increases occurring for the first 50 years. In the same species, Mäkinen et al. (2007) found that tracheid length continued to increase up to the age of the trees sampled (50 years), whereas tracheid width reached an asymptote at approximately 25 years. The model form we used was selected specifically to allow continued increases in length beyond the limits of our data. However, due to the relatively short rotations for loblolly pine, very little older material is commercially available and thus the models probably represent a significant proportion of the available resource that is used by the pulp and paper sector.

The model parameters estimated in this study are likely to be strongly influenced by our choice of sampling methods. Trees from the mean diameter class, and the classes (50 mm) immediately above and below the mean class were felled. Thus, our sample did not contain the smallest trees and largest trees within the stands. The consequences of this sampling strategy are likely evident in the random effects estimates, since the stand-level random effect accounted for an additional 9 percent

and 10 percent of the variation in tracheid length and width for the disk height models, respectively, while the tree-within-stand random effect accounted for very little additional variability (3 percent and 4 percent for tracheid width and tracheid length, respectively, over and above that explained by the fixed effects). Adding an effect of physiographic region to the model reduced the random effect of stand by 4 percent for tracheid length and width, with minimal changes in the tree random effect estimate. For Norway spruce, Chen et al. (2016) found that trees with lower growth rates had longer tracheids than fast-growing trees, and Jaakkola et al. (2005) found that increased thinning intensity was associated with a decrease in tracheid length, hence strategies that sample trees across the diameter distribution may result in higher random tree-within-stand variability. Dahlen et al. (2018) found that tree-within-stand accounted for an additional 6 percent of the variability in SG for loblolly pine, with data from a narrower range of stand conditions than sampled in the current study. Outside of loblolly pine, the impact of the random effects appears to be dependent on the species and the property in question. Auty et al. (2014) found that the random effect of tree explained over 10 percent of the variation in wood density models for Scots pine, and a little under 10 percent for MFA (Auty et al. 2013). For radiata pine, Moore et al. (2014) found the random effect of tree on the MFA of radiata pine was similar to the values found here for tracheid dimensions. Moore et al. (2015) found in radiata pine that the random effect of tree explained approximately 20 percent of the variability in spiral grain.

The differences in fibre properties across the southeastern United States growing regions closely follow previous regional variation results for loblolly pine whereby "improved" properties are found in trees near the southern coasts (Lower Coastal Plain, Gulf Coastal Plain, Upper Coastal Plain) versus trees grown further north and further inland (Hilly Coastal, Piedmont, North Atlantic) (Schimleck et al. 2018). This trend has been found by Jordan et al. (2007) for MFA, Jordan et al. (2008) and Antony et al. (2010) for SG, and Antony et al. (2011b) for MOE and MOR obtained from short clear samples. Loblolly pine growing near the southern coasts has a higher amount of latewood for a given cambial age than loblolly pine grown further north (Jordan et al. 2008; Samuelson et al. 2013). The increased amount of latewood is one reason why we found regional differences in tracheid length, because for a given annual ring, latewood tracheids are approximately 4 percent longer than earlywood tracheids (Buksnowitz et al. 2010). Jordan et al. (2008) hypothesized that the increased latewood near the southern coasts is due to higher number of degree days, warmer temperature, and increased precipitation that occurs in the late summer months. The variation in wood properties due to growing region is not unique to loblolly pine. In New Zealand, Cown and Ball (2001) attributed the regional variation in radiata pine wood density to the differences in latewood percent, while Kimberley et al. (2017) found regional differences in Douglas-fir (*Pseudotsuga menziesii* Mirb. Franco) wood density that were attributed to mean annual temperature differences.

The modelled stem maps show the within-tree variation of tracheid dimensions between juvenile corewood and outerwood, and mature corewood and outerwood that parallels the conceptual illustration put forth by Burdon et al. (2004). The radial variations are quite pronounced from the base of the modelled tree to the top; gradual shading in the lower 3 m of the profiles can be attributed to the so-called juvenile corewood, transitional (wood), and outerwood in the lower 3 m of the Burdon et al. (2004) illustrations. The tracheid length and width maps do not directly parallel tree maps constructed for SG for loblolly pine (Mora and Schimleck 2009; Dahlen et al. 2018), particularly for tracheid width where there is little property change with height. The trends by height are also reversed for tracheid length and width (with both increasing with height) when compared to SG, which typically decreases with height for a given cambial age (Auty et al. 2014; Dahlen et al. 2018). Given that lower MFA coincides with greater tracheid length (Brändström 2001; Hasegawa et al. 2010), it is not surprising the tracheid length map presented here more closely follows the pattern seen for MFA (Schimleck et al. 2018) than for SG. The different patterns of within-tree variability by wood property are related to the different types of morphological changes that occur in cells. New cells are created in the vascular cambium through cell division, followed by cell elongation and cell wall thickening (Nanayakkara et al. 2019). Cell elongation ceases when wall thickening occurs (Abe et al. 1997). The traditional concepts of juvenile and mature wood being associated with pith-to-bark variability is supported by the within-tree variation in wall thickness and SG. Burdon et al. (2004) discuss the need for a more detailed description of the within-tree variation in properties, preferring the terms "corewood" and "outerwood" to represent radial (i.e. pith-to-bark) variability, and "juvenile" and "mature" wood to represent the developing cambium that occurs with height in the tree. That is, wood formed at the stump and the pith is considered juvenile corewood, whereas higher in the stem (e.g. 10 m) the wood formed at the pith is considered mature corewood. The visual differences we see in wood properties maps appear to be related to whether a property is associated with cell wall elongation (MFA, tracheid length) or wall thickening (SG, wall thickness).

Longitudinal tracheids comprise over 90 percent of the cell volume in the secondary xylem for softwoods (Borovikov and Ugolev 1989). Because of the dual role that these tracheids have in providing water conduction and mechanical support, there are a number of hypotheses as to why the changes occur in their properties/dimensions (Lachenbruch et al. 2011). Mott et al. (2002) and Groom et al. (2000a,b) clearly show that tracheids produced at older cambial ages have significantly increased mechanical properties compared to tracheids produced at young ages. The increased mechanical properties with cambial age are needed in order for a tree to support its added weight as it grows, and to resist wind loads that increase with height growth (Lachenbruch et al. 2011, Hale et al. 2012, Gardiner et al. 2016, Dargahi et al. 2019). Regarding water transport, a compelling argument for why trees produce corewood with narrow tracheids, is that a young tree is more vulnerable to embolism because of the limited development of its root system which limits access to water during dry periods (Miller and Johnson 2017). Because of this increased vulnerability to embolism, trees produce corewood that is more resistant to embolism. For example, Domec and Gartner (2001) show that Douglas-fir corewood, with its narrower tracheids, loses 50 percent of its hydraulic conductivity at higher negative tensions (−4.7 MPa), compared to outerwood which loses 50 percent of its hydraulic conductivity at −3.5 MPa (−4.7 MPa is drier conditions than −3.5 MPa). As a tree establishes its root system, it gains access to more water, and due to the

increasing size of the tree, the tree in turn must pump more water to support the larger crown. Gartner (2006) calculated that as trees increased in size, water transport needs to increase by orders of magnitude in order to support the larger foliage area (up to 300 times). Here we find that tracheid width changes very little after 10 years, and thus hydraulic conductivity increases after 10 years is likely due to the increasing length of the tracheids, which results in water having to flow through fewer pits which decreases resistance to flow (Spicer and Gartner 1998).

The generation of mean tracheid length and width values based on a variety of simulated harvesting scenarios provides context to the pulp and paper industry for adjusting procurement strategies to account for variation in morphological fiber properties. Depending on product type, a facility may prefer chips from the outerwood, and tops, to obtain longer and wider tracheids, versus feedstock from forest thinnings. Nearly all of the pulp in the southeastern United States is produced from the Kraft process (Bentley and Steppleton 2013), which yields products such as linerboard, sack papers, fluff pulp, and dissolving pulp. For linerboard, tracheid coarseness is an important property, while tracheid length is important for sack papers and fluff pulp. For dissolving pulp, wood chemistry is likely more important than tracheid dimensions, although wood chemical composition and tracheid dimensions are clearly linked (Nabavi et al. 2018). Kibblewhite (1999) states that for radiata pine, the minimum tracheid length that pulp mills need to maintain is 2.05 mm to retain marketable tensile strength and bulk in the final paper product. Information for loblolly pine thresholds are not available, but all harvesting scenarios met this minimum length. While segregating material for tracheid length may be effective, doing so for width will likely not be effective because tracheid width varied little in the five scenarios simulated here. Similar conclusions were found by Havimo et al. (2008) for Norway spruce, who concluded that for tracheid width, the only meaningful distinction would be in separating between earlywood and latewood, which in practice is not feasible. While cell wall thickness was not measured in this study, products where thinner cell walls are desirable would favor tree tops over wood chips procured from sawmills because SG, and thus wall thickness, decreases with height for loblolly pine (Dahlen et al. 2018; Schimleck et al. 2020).

A limitation of the models developed here is the inability to differentiate earlywood and latewood tracheids, as well as to delineate relatively narrow rings. This is because we used a fixed window size of 10 mm for the NIR spectroscopy. A finer resolution could have been achieved at the expense of model accuracy. Using the same NIR spectrometer setup, Jones et al. (2007) found that prediction accuracy decreased with smaller sampling windows. They also reported that increased scanning resolution made the organization of spectra significantly more challenging because the NIR spectrometer is not directly linked to the radial scanning equipment. Equipment that is specifically designed for linear scanning, such as line scan hyperspectral imaging systems, would have great potential for use in describing and predicting wood property radial variability, since these systems allow for within-ring separation of earlywood and latewood properties to be estimated. The latter can be achieved because hyperspectral systems combine NIR spectroscopy with imaging, so within-ring variation can be predicted. Using such a system would represent a significant improvement over the 10 mm resolution used in this study. Separating the earlywood and latewood tracheid properties would also enable improved links between anatomical properties and water transport (Domec and Gartner 2002) because for a given annual ring, latewood tracheids are longer than earlywood tracheids (Taylor and Burton 1982; Buksnowitz et al. 2010).

Conclusions

In this study, we present the first modelled tracheid length and tracheid width from data collected from macerated tracheids and near-infrared spectroscopy calibration models for loblolly pine obtained from managed plantations. Nonlinear mixed-effects models were constructed to quantify the variation in these properties that occurs within trees. The fixed effects of the models explained 71 percent of the variation for tracheid length, and 57 percent of the variation for tracheid width. Significant regional differences were found, with larger asymptotic values for tracheid length and width for trees growing near the southern coasts. Two-dimensional whole-tree maps of tracheid dimension were constructed showing changes in tracheid length and width with tree age. Whole-tree tracheid length increased from 2.24 mm at age 12, to 2.51 mm at age 18 and to 2.73 mm at age 25. Whole-tree tracheid width increased from 40.5 μm at age 12, to 41.3 μm at age 18, to 41.8 μm at age 25. The tops of trees at age 25 had similar tracheid length and width (2.46 mm, 41.0 μm) as the whole-tree average at age 18. Chips generated from the outermost wood of sawlogs at age 25 had the highest tracheid length (3.13 mm) and width (42.5 μm) amongst the five simulated product scenarios that were compared. Models that predict variability in wood and fibre properties are needed in order to better understand the available plantation resource, and the models developed here could be integrated into growth and yield systems or procurement systems to predict tracheid properties for loblolly pine. The five product scenarios shown here at different ages and positions within the tree demonstrate an application that the pulp and paper or the forest products industries could use to improve resource assessment to meets the needs for current and future products.

Acknowledgements

We would like to thank the reviewers and the editor, Dr. Gary Kerr, for their helpful comments and suggestions in improving the manuscript.

Funding

The work was supported by the Wood Quality Consortium (WQC) at the University of Georgia, the NIFA McIntire-Stennis project 1006098, and the National Science Foundation (NSF) Center for Advanced Forest Systems (CAFS).

Conflict of interest statement

None declared.

References

Abe, H., Funada, R., Ohtani, J. and Fukazawa, K. 1997 Changes in the arrangement of cellulose microfibrils associated with the cessation of cell expansion in tracheids. *Trees* **11**, 328–332.

Antony, F., Schimleck, L.R., Daniels, R.F., Clark, A. III and Hall, D.B. 2010 Modeling the longitudinal variation in wood specific gravity of planted loblolly pine (Pinus taeda) in the United States. *Can J Forest Res* **40**, 2439–2451.

Antony, F., Schimleck, L.R., Jordan, L., Clark, A. III and Daniels, R.F. 2011a Effect of early age woody and herbaceous competition control on wood properties of loblolly pine. *For Ecol Manage* **262**, 1639–1647.

Antony, F., Jordan, L., Schimleck, L.R., Clark, A. III, Souter, R.A. and Daniels, R.F. 2011b Regional variation in wood modulus of elasticity (stiffness) and modulus of rupture (strength) of planted loblolly pine in the United States. *Can J For Res* **41**, 1522–1533.

Auty, D., Gardiner, B.A., Achim, A., Moore, J.R. and Cameron, A.D. 2013 Models for predicting microfibril angle variation in scots pine. *Ann For Sci* **70**, 209–218.

Auty, D., Achim, A., Macdonald, E., Cameron, A.D. and Gardiner, B.A. 2014 Models for predicting wood density variation in scots pine. *Forestry* 449–458.

Baddeley, A., Rubak, E. and Turner, R. 2016 *Spatial point patterns: methodology and applications with R*. Chapman and Hall/CRC Press, England, p. 810 9781482210200.

Bentley, J.W. and Steppleton, C.D. 2013 Southern pulpwood production, 2011. In *United States Department of Agriculture Forest Service Southern Research Station Resource Bulletin SRS-194*.

Brändström, J. 2001 Micro- and ultrastructural aspects of Norway spruce tracheids: A review. *IAWA J* **22**, 333–353.

Briggs, D.G. 2010 Enhancing forest value productivity through fiber quality. *J Forestry* **108**, 174–182.

Borovikov, A.M. and Ugolev, B.N. 1989 *The hand-book of wood (in Russian)*. Lesnaya Promiselennost, Moscow, 296 pp.

Buksnowitz, C., Teischinger, A., Grabner, M., Müller, U. and Mahn, L. 2010 Tracheid length in Norway spruce (*Picea abies* (L.) karst.) analysis of three databases regarding tree age, cambial age, tree height, inter-annual variation, radial distance to pith and log qualities. *Wood Research* **55**, 1–14.

Bullock, B.P. and Burkhart, H.E. 2001 Equations for predicting green weight of loblolly pine trees in the south. *South J Appl For* **27**, 153–159.

Burdon, R.D., Kibblewhite, R.P., Walker, J.C.F., Megraw, R.A., Evans, R. and Cown, D.J. 2004 Juvenile versus mature wood: A new concept, orthogonal to corewood versus outerwood, with special reference to Pinus radiata and P-taeda. *Forest Sci* **50**, 399–415.

Burkhart, H.E. and Tomé, M. 2012 *Modeling Forest Trees and Stands*. Springer-Verlag, Berlin, Germany, pp. 405–427 978-90-481-3170-9.

Carvalho, M.G., Ferreira, P.J., Martins, A.A. and Figueiredo, M.M. 1997 A comparative study of two automated techniques for measuring fiber length. *TAPPI J* **80**, 137–142.

Chen, Z.Q., Karlsson, B., Mörling, T., Olsson, L., Mellerowicz, E.J., Wu, H.X. *et al*. 2016 Genetic analysis of fiber dimensions and their correlation with stem diameter and solid-wood properties in Norway spruce. *Tree Genet Genomes* **12**, 123.

Çöpür, Y., Makkonen, H. and Amidon, T.E. 2005 The prediction of pulp yield using selected fiber properties. *Holzforschung* **59**, 477–480.

Cown, D.J. and Kibblewhite, R.P. 1980 Effects of wood quality variation in New Zealand radiata pine on Kraft fiber properties. *New Zeal J For Sci* **10**, 521–532.

Cown, D.J. and Ball, R.D. 2001 Wood densitometry of 10 Pinus radiata families at seven contrasting sites: Influence of tree age, site and genotype. *New Zeal J For Sci* **31**, 88–100.

Dahlen, J., Auty, D. and Eberhardt, T.L. 2018 Models for predicting specific gravity and ring width for loblolly pine from intensively managed plantations, and implications for wood utilizations. *Forests* **9**, 292.

Dargahi, M., Newson, T. and Moore, J. 2019 Buckling behaviour of trees under self-weight loading. *Forestry* **92**, 393–405.

Diéguez-Aranda, U., Burkhardt, H.E. and Amateis, R.L. 2006 Dynamic site model for loblolly pine (*Pinus taeda* L.) plantations in the United States. *Forest Sci* **52**, 262–272.

Domec, J.C. and Gartner, B.L. 2001 Cavitation and water storage capacity in bole xylem segments of mature and young Douglas-fir trees. *Trees* **15**, 204–214.

Domec, J.C. and Gartner, B.L. 2002 How do water transport and water storage differ in coniferous earlywood and latewood? *J Exp Botany* **53**, 2369–2379.

Evans, R. 1994 Rapid measurement of the transverse dimensions of tracheids in radial wood sections from *Pinus radiata*. *Holzforschung* **48**, 168–172.

Evans, R., Kibblewhite, R.P. and Stringer, S. 1997 Kraft pulp fibre property prediction from wood properties in eleven radiata pine clones. *Appita J* **50**, 25–33.

Evans, R., Kibblewhite, R.P. and Lausberg, M. 1999 Relationships between wood and pulp properties of twenty-five 13 year old radiata pine trees. *Appita J* **52**, 132–139.

Fox, T.R., Jokela, E.J. and Allen, H.L. 2007 The development of pine plantation silviculture in the southern United States. *J For* **105**, 337–347.

Franklin, G. 1945 Preparation of thin sections of synthetic resins and wood-resin composites, and a new macerating method for wood. *Nature* **155**, 51–55.

Gardiner, B., Berry, P. and Moulia, B. 2016 Review: Wind impacts on plant growth, mechanics and damage. *Plant Sci* **245**, 94–118.

Gartner, B.L. 2006 Prediction of wood structural patterns in trees by using ecological models of plant water relations. In *Characterization of the Cellulosic Cell Wall*. D.D., Stokke, L.H., Groom (eds.). Wiley-Blackwell, Hoboken, United States, pp. 38–52.

Gogoi, B.R., Sharma, M. and Sharma, C.L. 2018 Tracheid length variation in *Pinus kesiya* Royle ex. Gord. As affected by age, distance from pith, growth rate, and ring width. *J Tree Sci* **37**, 55–61.

Gräler, B., Pebesma, E. and Heuvelink, G. 2016 Spatio-temporal interpolation using gstat. *R J* **8**, 204–218.

Gray, J.A., Bentley, J.W., Cooper, J.A. and Wall, D.J. 2018 Southern pulpwood production, 2016. In *United States Department of Agriculture Forest Service Southern Research Station e-Resource Bulletin SRS-222*.

Groom, L., Mott, L. and Shaler, S. 2002a Mechanical properties of individual southern pine fibers. Part I. determination and variability of stress-strain curves with respect to tree height and juvenility. *Wood Fiber Sci* **34**, 14–27.

Groom, L., Shaler, S. and Mott, L. 2002b Mechanical properties of individual southern pine fibers. Part III. Global relationships between fiber properties and fiber location within an individual tree. *Wood Fiber Sci* **34**, 238–250.

Hale, S.E., Gardiner, B.A., Wellpott, A., Nicoll, B.C. and Achim, A. 2012 Wind loading of trees: Influence of tree size and competition. *Eur J Forest Res* **131**, 203–217.

Hasegawa, M., Takata, M., Matsumura, J. and Oda, K. 2010 Effect of wood properties on within-tree variation in ultrasonic wave velocity in softwood. *Ultrasonics* **51**, 296–302.

Havimo, M., Rikala, J., Sirviö, J. and Sipi, M. 2008 Distributions of tracheid cross-sectional dimensions in different parts of Norway spruce stems. *Silva Fennica* **42**, 89–99.

Hayatgheibi, H., Fries, A., Kroon, J. and Wu, H.X. 2019 Genetic analysis of fiber-dimension traits and combined selection for simultaneous improvement of growth and stiffness in lodgepole pine (*Pinus contorta*). *Can J For Res* **49**, 500–509.

Hijmans, R.J. raster: *Geographic data analysis and modeling*. 2016. R package version 2.5-8. https://CRAN.R-project.org/package=raster

Hirn, U. and Bauer, W. 2006 A review of image analysis based methods to evaluate fiber properties. *Lenzinger Berichte* **86**, 96–105.

Jaakkola, T., Mäkinen, H., Sarén, M.-P. and Saranpää, P. 2005 Does thinning intensity affect the tracheid dimensions of Norway spruce? *Can J For Res* **35**, 2685–2697.

Jones, P.D., Schimleck, L.R., So, C.L., Clark, A. III and Daniels, R.F. 2007 High resolution scanning of radial strips cut from increment cores by near infrared spectroscopy. *IAWA J* **28**, 473–484.

Jordan, L., He, R., Hall, D.B., Clark, A. III and Daniels, R.F. 2007 Variation in loblolly pine ring microfibril angle in the Southeastern United States. *Wood Fiber Sci* **39**, 352–363.

Jordan, L., Clark, A. III, Schimleck, L.R., Hall, D.B. and Daniels, R.F. 2008 Regional variation in wood specific gravity of planted loblolly pine in the United States. *Can J Forest Res* **38**, 698–710.

Kibblewhite, R.P. 1980 Radiata pine corewood and slabwood, and their interrelations with pulp and handsheet properties. *NZ J For Sci* **10**, 533–550.

Kibblewhite, R.P., Evans, R. and Riddell, M.J.C. 1997 Handsheet property prediction from Kraft-fibre and wood-tracheid properties in eleven radiata pine clones. *Appita J* **50**, 131–138.

Kibblewhite, R.P. 1999 Designer fibres for improved papers through exploiting genetic variation in wood microstructure. *Appita J* **52**, 429–435,440.

Kibblewhite, R.P. and Evans, R. 2001 Dimensions relationships among radiata pine wood tracheid, and chemical and TMP pulp fibres. *Appita J* **54**, 297–303.

Kibblewhite, R.P., Evans, R. and Riddell, M.J.C. 2003 Kraft handsheet, and wood tracheid and chemical property interrelationships for 50 individual radiata pine trees. *Appita J* **56**, 229–233.

Kimberley, M.O., McKinley, R.B., Cown, D.J. and Moore, J.R. 2017 Modelling the variation in wood density of New Zealand grown Douglas-fir. *NZ J For Sci* **47**, 15.

Lachenbruch, B., Moore, J.R. and Evans, R. 2011 Radial variation in wood structure and function in woody plants, and hypotheses for its occurrence. In *Size- and Age-Related Changes in Tree Structure and Function*. F.C., Meinzer, B., Lachenbruch, T.E., Dawson (eds.). Springer-Verlag, Berlin, Germany, pp. 121–164.

Lindström, H. 1997 Fiber length, tracheid diameter, and latewood percentage in Norway spruce: Development from pith outwards. *Wood Fiber Sci* **29**, 21–34.

Lindström, H. 2002 Intra-tree models of juvenile wood in Norway spruce as an input to simulation software. *Silva Fennica* **36**, 521–534.

Mäkinen, H., Jaakkola, T., Piispanen, R. and Saranpää, P. 2007 Predicting wood and tracheid properties of Norway spruce. *For Ecol Manage* **241**, 175–188.

McKeand, S., Mullin, T., Bryam, T. and White, T. 2003 Deployment of genetically improved loblolly and slash pines in the south. *J Forest* **101**, 32–37.

McKenzie, A.W. 1994 *A Guide to Pulp Evaluation*. CSIRO.

Megraw, R.A. 1985 *Wood quality factors in loblolly pine*. TAPPI, United States, p. 88.

Miller, M.L. and Johnson, D.M. 2017 Vascular development in very young confier seedlings: Theoretical hydraulic capacities and potential resitance to embolism. *Am J Bot* **104**, 1–14.

Moore, J.R., Cown, D.J. and McKinley, R.B. 2014 Modelling microfibril angle variation in New Zealand-grown radiata pine. *NZ J For Sci* **44**, 25.

Moore, J.R., Cown, D.J. and McKinley, R.B. 2015 Modelling spiral grain angle variation in New Zealand-grown radiata pine. *NZ J For Sci* **45**, 15.

Moore, J.R. and Cown, D.J. 2017 Corewood (juvenile wood) and its impact on wood utilisation. *Curr Forestry Rep* **3**, 107–118.

Mora, C.R., Allen, H.L., Daniels, R.F. and Clark, A. III 2007 Modeling corewood-outerwood transition in loblolly pine using wood specific gravity. *Can J For Res* **37**, 999–1011.

Mora, C.R. and Schimleck, L.R. 2009 Determination of within-tree variation of *Pinus taeda* wood properties by near infrared spectroscopy. Part 2: Whole-tree wood property maps. *Appita J* **62**, 232–238.

Mott, L., Groom, L. and Shaler, S. 2002 Mechanical properties of individual southern pine fibers. Part II. Comparison of earlywood and latewood fibers with respect to tree height and juvenility. *Wood Fiber Sci* **34**, 221–237.

Nabavi, M., Dahlen, J., Schimleck, L., Eberhardt, T.L. and Montes, C. 2018 Regional calibration models for predicting loblolly pine tracheid properties using near-infrared spectroscopy. *Wood Sci Technol* **52**, 445–463.

Nanayakkara, B., Dickson, A.R. and Meason, D.F. 2019 Xylogenesis of *Pinus radiata* D. don growing in New Zealand. *Ann For Sci* **76**, 74.

Paavilainen, L. 1993 Importance of cross-dimensional fibre properties and coarseness for the characterisation of softwood sulphate pulp. *Paperi ja Puu* **75**, 343–351.

Ratkowsky, D.A. 1990 *Handbook of nonlinear regression models*. Marcel Dekker, New York, 241 p.

R Core Team. 2019 *R: A language and environment for statistical computing*. R Foundation for Statistical Computing, Vienna, Austria. URL http://www.R-project.org/.

RStudio. 2019 *RStudio: Integrated development environment for R*. Boston, MA. https://www.rstudio.com/

Pebesma, E.J. 2004 Multivariable geostatistics in S: The gstat package. *Comput Geosci* **30**, 683–691.

Pinherio, J.C. and Bates, D.M. 2000 *Mixed-effects models in S and S-Plus*. Springer, New York.

Pinheiro, J., Bates, D., DebRoy, S., Sarkar, D. and R Core Team 2016 Nlme: Linear and nonlinear mixed effects models. *R package version 3.1–128* . https://CRAN.R-project.org/package=nlme.

Pulkkinen, I., Ala-Kaila, K. and Aittamaa, J. 2006 Characterization of wood fibers using fiber property distributions. *Chem Eng Process* 45546–45554.

Samuelson, L.J., Eberhardt, T.L., Bartkowiak, S.M. and Johnsen, K.H. 2013 Relationships between climate, radial growth and wood properties of mature loblolly pine in Hawaii and a northern and southern site in the southeastern United States. *For Ecol Manage* **310**, 786–795.

Scallan, A.M. and Green, H.V. 1975 The effect of pulping upon the dimensions of wood tracheids. *Wood Fiber Sci* **7**, 226–233.

Schimleck, L.R., Jones, P.D., Peter, G.F., Daniels, R.F. and Clark III, A. 2004 Nondestructive estimation of tracheid length from sections of radial wood strips by near infrared spectroscopy. *Holzforschung* **58**, 375–381.

Schimleck, L.R., Antony, F., Dahlen, J. and Moore, J. 2018 Wood and fiber quality of plantation-grown conifers: A summary of research with an emphasis on loblolly and radiata pine. *Forests* **9**, 298.

Schimleck, L.R., Antony, F., Mora, C. and Dahlen, J. 2020 *Whole-tree tracheid property maps for loblolly pine at different ages*. Wood Sci Technol In Press.

Snee, R.D. 1977 Validation of regression models: Methods and examples. *Technometrics* **19**, 415–428.

Spicer, R. and Gartner, B.L. 1998 Hydraulic properties of Douglas-fir (*Pseudotsuga menziesii*) branches and branch halves with reference to compression wood. *Tree Physiol* **18**, 777–784.

Taylor, F.W. and Burton, J.D. 1982 Growth ring characteristics, specific gravity, and fiber length of rapidly grown loblolly pine. *Wood Fiber Sci* **14**, 204–210.

Via, B.K., Stine, M., Shupe, T.F., So, C.L. and Groom, L. 2004 Genetic improvement of fiber length and coarseness based on paper product performance and material variability – A review. *IAWA J* **25**, 401–414.

Via, B.K., Shupe, T.F., Stine, M., So, C.L. and Groom, L. 2005 Tracheid length prediction in Pinus palustris by means of near infrared spectroscopy: The influence of age. *Holz als Roh-und Werkstoff* **63**, 231–236.

White, D.E., Courchene, C., McDonough, T., Schimleck, L., Jones, D., Purnell, R. *et al.* 2009 Effects of specific gravity and wood chemical content on the pulp yield of loblolly pine. *TAPPI J* **92**, 29–34.

Wickham, H. 2009 *ggplot2: Elegant graphics for data analysis*. Springer-Verlag, New York.

Wickham, H., Francois, R. 2017 tidyverse. R package version . https://CRAN.R-project.org/package=tidyverse

Zhao, D., Kane, M.B., Teskey, R.O., Fox, T.R., Albaugh, T.J., Allen, H.L. *et al.* 2016 Maximum response of loblolly pine plantations to silvicultural management in the southern United States. *For Ecol Manage* **375**, 105–111.

Zobel, B. and Sprague, J. 1998 *Juvenile wood in trees*. Springer, New York.